Forced Air Convection in Additively Manufactured Lattice Structures

John Wallace, Kevin Laux, Albert To

Introduction

The purpose of this experiment was to better understand heat transfer properties of specific lattice structures shown in Figure 1.

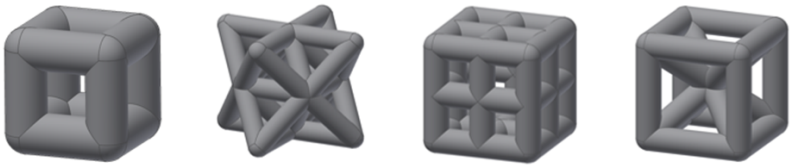

Figure 1: Cubic, octet, midpoint, and diagonal lattice structures.

Cubes consisting of 512 unit cells (8x8x8) were created on an EOS M290 3D printer from an aluminum alloy powder. For the cubic lattice, additional samples were printed with various relative densities and lattice orientations. Data was collected over a range of flow rates and electrical input powers for each lattice. Concurrently with thermal data, the pressure drop across each sample was found.

Methods

The experimental set up used to collect data on the samples is shown below.

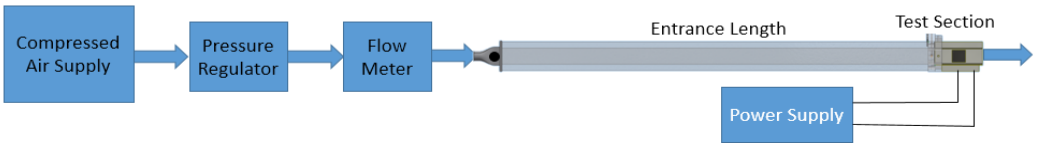

Figure 2: Outline of the experimental set up.

The air regulator regulates air before being flowed into the entrance length at a rate determined by the flow meter. Temperature readings are made at the beginning of the entrance length and inside the test section by T-type thermocouples indicated by black dots in Figure 3.

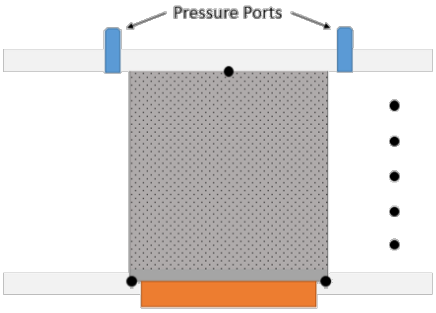

Figure 3: Layout of the test section.

The samples are loaded into the test section and heated by the plate shown in orange in Figure 3. Air flows through the entrance length of 24.5 diameters at which point velocity measurements are taken using a hotwire anemometer. Measurements are taken in the

vertical and diagonal directions every .0625". Pressure data is collected on the samples with a manometer by raising the flow rate from 2 SCFM to 14 SCFM and recording the high and low over 30 second intervals for every 1 SCFM. Thermal data was collected by holding the input power at a constant 60.4W and decreasing the flow rate by 2 SCFM from 14 SCFM to 2 SCFM. A second set of data was collected by holding the base temperatures constant at 60C and varying the input power for each flow rate. Some samples tested in this experiment are shown below in Figure 4. Each sample has a relative density of 40, with the exception of cubic structures.

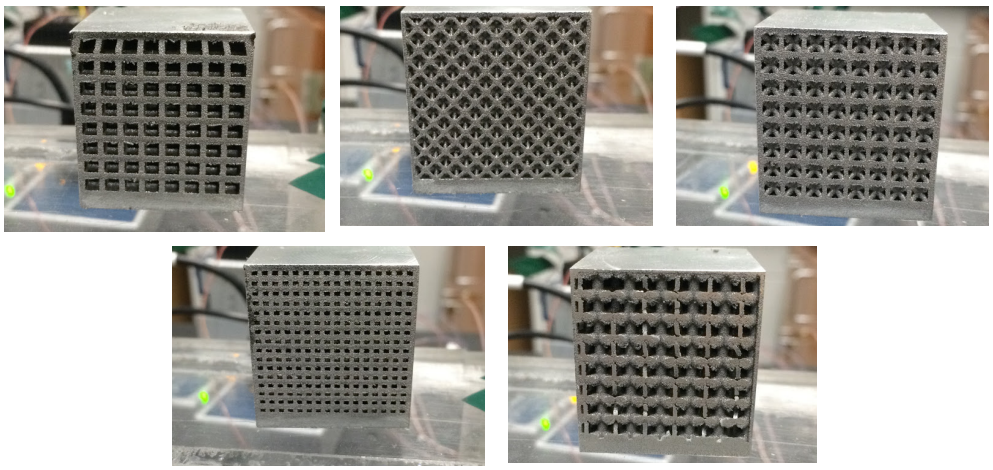

Figure 4: (from top left to bottom right) Cubic 20, octet, diagonal, midpoint, cubic with 45º orientations.

Velocity Analysis

To begin analyzing the velocity measurements the results of these tests are plotted in the Figure below and overlaid against the results published by Melling and Whitelaw[1], which agree with our data well.

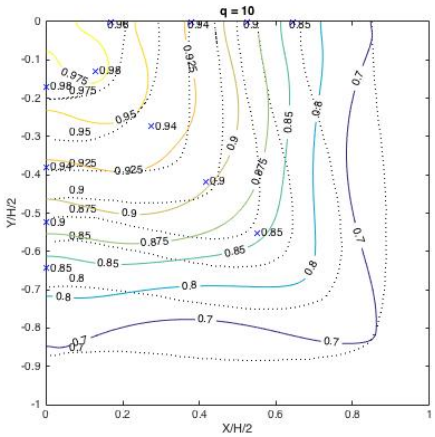

Figure 5: Normalized velocity profile results for 10 SCFM plotted against the Melling and Whitelaws results at 36.8 hydraulic diameters shown as dotted lines.

The velocity data collected was then interpolated into a surface using Matlab and integrated according to the equation for volume flow.

$$Q = \iint v \, dA \tag{1}$$

This data is shown in the table below. As expected the percent error decreases with increasing air velocity due to the hot wire anemometers irregular results at low velocities[2].

Measured Flow Rate (SCFM)	Calculated Flow Rate (SCFM)	Error
2	3.26	63.09%
5	5.50	9.88%
8	8.73	9.10%
10	10.53	5.30%

Figure 6: Results of the volume flow calculations conducted in Matlab.

Pressure Drop

Following the analysis of the airflow in the duct it was important to look at the pressure drop across each type of structure. As the relative density of cubic structures increases the pressure drop can be seen to increase with it. The reduction of flow area and increase of internal surface area explains this relationship.

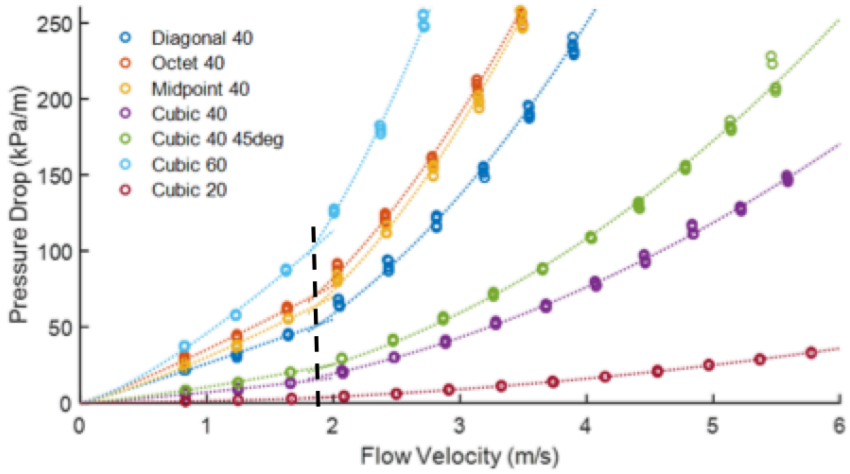

Figure 7: Pressure drop plotted against flow velocity for the range of samples.

The pressure drop results can be plotted according to the equation

$$\Delta P = aV^b \tag{2}$$

with the variables a and b taking values according to the 2 regimes indicated by the dashed line in Figure 7

Lattice Structure	Low Velocity Fit		High Velocity Fit	
	a	b	a	b
Diagonal 40	25.90	1.09	13.72	2.09
Octet 40	35.14	1.14	19.76	2.06
Midpoint 40	30.10	1.21	16.03	2.21
Cubic 40	7.01	1.23	4.88	1.98
Cubic 40 45deg	10.51	1.27	5.95	2.09
Cubic 60	45.81	1.31	25.51	2.28
Cubic 20	1.27	1.54	1.01	1.99

Figure 8: The values of a and b for equation 2.

Thermal Resistance

After collecting thermal data at a constant power of 60.4W and calculating thermal losses, it was clear that losses were prevalent across structures. Due to the nature of the cells and the range of base operating temperatures it came into question whether each structure experienced different losses. In order to investigate these losses and see consistency across structures, data was recollected while holding the base temperatures at a constant temperature of 60˚C. It was found that the differences in base temperatures across structures did not contribute to a significant difference in losses.

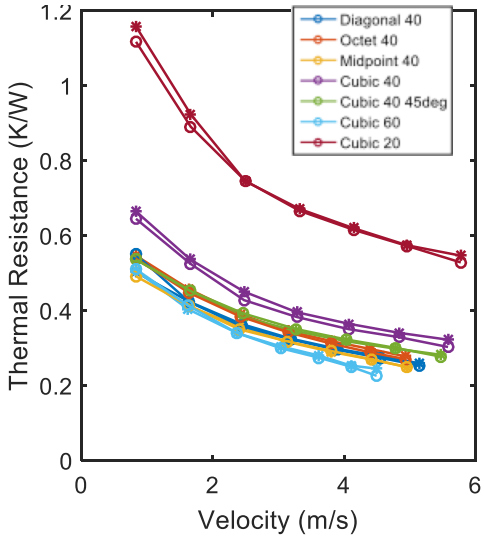

Figure 9: Plot of Thermal resistance as a function of velocity. Circles represent results from tests conducted at constant power while stars represent trials conducted at constant temperature. These tests are seen to be consistent with each other.

By looking at the differences in the cubic structures in Figure 9 it is clear that increasing the density decreases the thermal resistance calculated by equation 3.

$$R_{th} = \frac{T_{surface} - T_{fluid}}{q_{heat}} \tag{3}$$

Furthermore, since each lattice structure has a relative density of 40 it is valuable to note that one can achieve a lower thermal resistance at the same density by using a different unit cell.

Conclusion

Reviewing the findings from thermal resistance calculations allows for conclusions to be drawn about effective heat transfer structures. When comparing the pumping power vs. thermal resistance the most effective structures will be those with the lowest pumping power and thermal resistance in Figure 10.

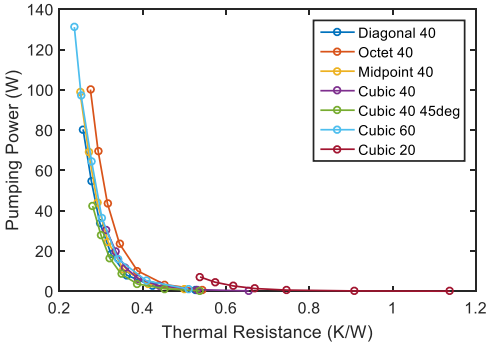

Figure 10.

Therefore the structures with points closest to the origin will be the most efficient when looking at amount of power needed to dissipate a certain amount of heat. These can be seen in Figure 11, which provides a normalized distance from the origin for each structure at various pumping powers.

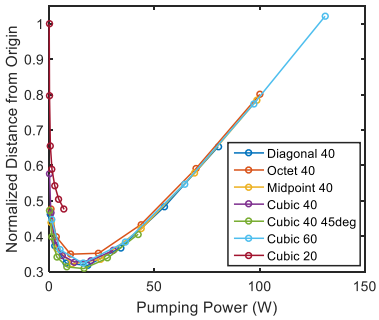

Figure 11.

Future Research

This project will see continued growth in the coming months. Recently seven new samples were printed on the EOS M290. These new samples provide additional relative density samples for the cubic structure as well as samples with density gradients across the structure. These density gradients will allow for additional testing on the effect that orientation has on convective heat transfer. Furthermore, another experimental set up has been designed which will allow for thermal conductivity tests to be run on the samples.

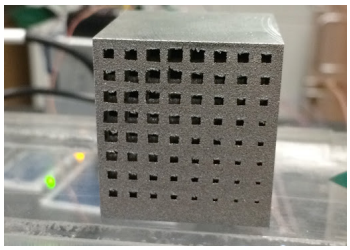

Figure 12: A new sample with a density gradient

Bibliography

1. Melling, A., & Whitelaw, J. H. (1976). Turbulent flow in a rectangular duct.*Journal of Fluid Mechanics*, *78*(02), 289. doi:10.1017/s0022112076002450
2. Christman, P. J., & Podzimek, J. (1981). Hot-wire anemometer behaviour in low velocity air flow. *Journal of Physics E: Scientific Instruments*, *14*(1), 46–51. doi:10.1088/0022-3735/14/1/013